HIGH-RESOLUTION NMR SPECTROSCOPY ON A CHIP BY STRUCTURAL COMPENSATION OF MAGNETIC SUSCEPTIBILITY MISMATCH

Herbert Ryan[1,2], James P. Landers[1,2,3], Matthew R. Begley[4], and Marcel Utz[5]

[1]*Center for Microsystems for the Life Sciences,* [2]*Department of Mechanical and Aerospace Engineering and* [3]*Department of Chemistry, University of Virginia, Charlottesville, VA, USA*

[4]*Department of Mechanical Engineering, University of California, Santa Barbara, CA, USA*

[5]*School of Chemistry, University of Southampton, UK*

ABSTRACT

Microfluidic compensation structures are introduced as a tool to homogenize magnetic field gradients present in microfluidic NMR spectroscopy. Magnetic field distortions are eliminated by compensating the magnetic susceptibility mismatch between the sample fluid and chip material through additional, lithographically defined compensation structures. This strategy will allow high resolution NMR spectroscopy on a chip, enabling a range of metabolomic applications.

KEYWORDS: Nuclear magnetic resonance, Spectroscopy, Inductive Coupling, Metabolomics, Structural shimming

INTRODUCTION

The goal of this work is to improve the resolution of microfluidic nuclear magnetic resonance spectroscopy. NMR spectroscopy is widely applied to the study of biological molecules in a variety of contexts. Of particular interest here is its capability to resolve the constituents of complex metabolic mixtures containing dozens to hundreds of compounds at µM levels. Medical diagnostics based on NMR metabolomic analysis (so far, of macroscopic samples) is a rapidly developing field, with a large number of diagnostic assays emerging [1]. At the same time, microfluidic devices offer convenient and efficient possibilities for sample separation and preparation. Combining the two approaches would empower microfluidic assays with the resolution and specificity of NMR spectroscopy [2].

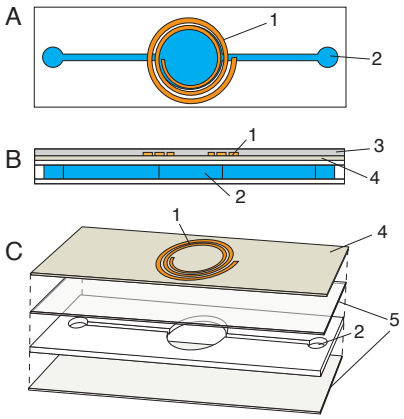

***Figure 1**: Principle of microfluidic NMR chips. A: top view; B: side view; C: RF resonator (1) is layered above the sample volume (2)*

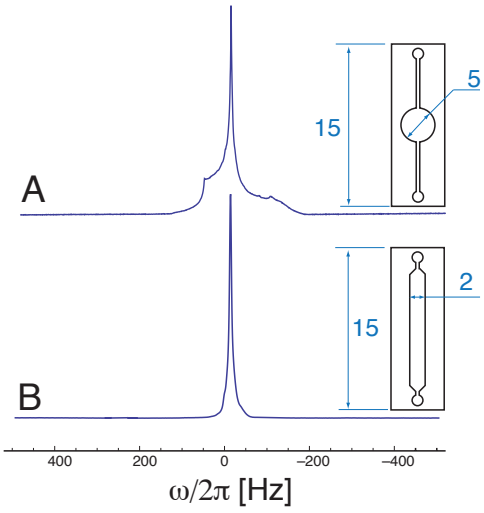

***Figure 2**: A: spectral line shape obtained from PMMA chip with circular sample chamber. Severe susceptibility broadening is obvious. B: A rectangular sample chamber gives much better resolution.*

There are two main challenges in the design of any NMR probe hardware: sensitivity and resolution. In probing biological samples, very complex spectra can be encountered making resolution paramount to deciphering chemical makeup. Improvements to sensitivity alone will not alleviate this problem as broad spectral lines tend to overlap. In microfluidic systems, magnetic susceptibility mismatch between the chip/capillary material and the sample is usually the dominant source of line broadening.

A number of miniaturized NMR systems have been explored [2-9] with line widths in the 3-10 ppb range. In virtually all cases so far, this has been achieved by severely restricting the device geometry to a cylinder or a linear strip (see figure 1). Our approach removes this constraint by adding lithographically defined shimming compensation structures. This preserves the non-invasive nature of NMR spectroscopy, without the need to extract the sample from the chip and inject into a dedicated capillary NMR probe. Since the compensation structures are made at the same time as the fluidic network, they add no manufacturing cost to the system.

Figure 2 shows the line shape of a water spectrum at 600 MHz from two planar microfluidic chips using an inductively coupled resonator [7,8]. It is obvious that the shape of sample chamber profoundly influences the line shape. The circular sample (A) produces a very broad (>200 Hz) line with a highly non-Lorentzian shape. This would make it very difficult to resolve individual compounds in a metabolic mixture. The longitudinal sample chamber shown in Fig. 2B produces a much sharper line. The goal of the present work is to produce sharp lines from sample chambers with small aspect ratios such as the one in Fig. 2A.

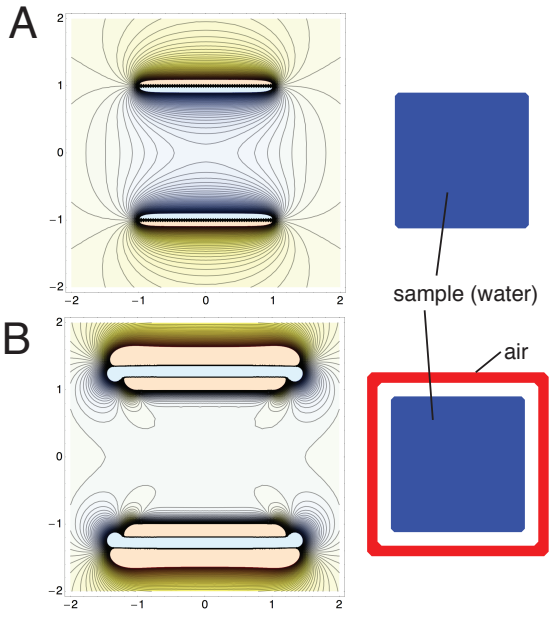

***Figure 3**: Calculated magnetic field distribution in a microfluidic chip (center of sample volume plane); sample chamber 4 x 4 mm; 150 µm depth. A: sample chamber only; B: sample chamber plus surrounding air-filled compensation structure. Iso-field lines are separated by 1 ppb.*

THEORY

Microfluidic chips are usually fabricated from diamagnetic materials such as glass, poly(styrene), or PDMS. The magnetic susceptibilities of such materials lie in the range of –11 to –6 ppm. Typically, the chip material's susceptibility differs from that of the sample fluid (–9.05 ppm in the case of water) by several hundred parts per billion (ppb). As shown in the computed field maps of Figure 3A, this leads to strong variations of the magnetic field inside the sample volume, causing line broadening and loss of resolution. Figure 2A shows the spectrum of water obtained with a round sample chamber in a 600 MHz NMR spectrometer. The field distortions lead to a broad line with a foot of more than 200 Hz width. Using a long rectangular sample chamber reduces the line width (Fig 2B), but at the expense of reduced sensitivity, since only the center part of the sample volume contributes to the signal. The distribution of the demagnetizing field in a rectangular sample chamber based on a 2 ppm mismatch between the chip material and the sample has been calculated using a 2D moment method. As shown in Fig. 3A, the field is very inhomogeneous inside the sample chamber. Figure 3B shows the resulting field lines produced when surrounding the sample chamber with a secondary structure containing a material with magnetic susceptibility offset from the base material opposite to that of the sample. The demagnetizing field has been largely eliminated from the inside of the sample, leading to field that is constant to within 1 ppb over the vast majority of the sample space.

EXPERIMENTAL

Microfluidic devices were fabricated by dichloromethane bonding of three poly(methyl methacrylate) (PMMA) layers. A standard engraving Versa Laser (model VLS3.50) was employed to Pattern PMMA sheets. Resonators were etched from pre-fabricated polyimide foil covered with 28 um of Cu (Upisel, UBE Industries, Inc.). The resonator structure was then sandwiched between an additional PMMA layer. This ensured that the structure is exposed to a well-defined dielectric, therefore improving the stability of the self-resonance frequency. Fully assembled chips were then filled with the solution of interest, taking particular care not to allow bubbles in close proximity to the sample chamber. The surrounding compensation chambers contained trace amounts of evaporated ethanol and dichloromethane (used in the bonding process) along with air. Chips were then inserted to a specially fabricated holder to ensure repeatability between multiple samples. The collective chip and holder were then inserted into a Doty 12mm microimaging probe. Experiments were conducted with a Varian 600 MHz NMR spectrometer, with a static field strength of 14.1 T. Liquid state NMR measurements were conducted using a dedicated probe head with a symmetric pair of single loop inductors of 10mm diameter (Figure 2). Resonators were fixed to a microfluidic chip containing a rectangular sample chamber of 15 µl total vol-

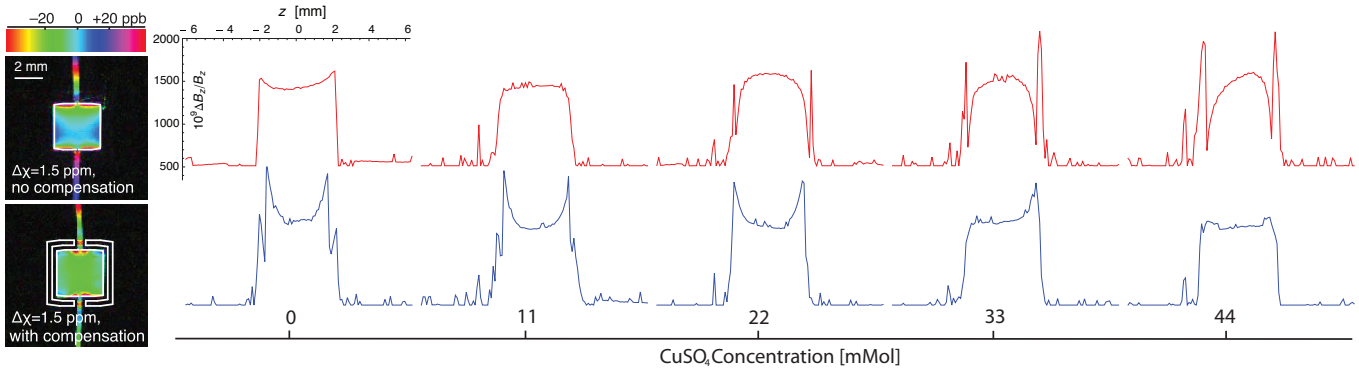

***Figure 4:** (left) Experimental MRI field maps and (right) vertical field profiles through the center lines with varying susceptibility mismatches. Top row: susceptibility between chip and sample is mismatched at higher $CuSO_4$ concentrations in H_2O. Bottom row: matching at higher $CuSO_4$ concentration corresponds to the presence of the compensation structure.*

ume, with a volume of 4 µl exposed to the rf field of the microcoil. The probe efficiency and rf homogeneity were tested by recording nutation sequences of water doped with 2mM of $CuSO_4$. Spectral resolution was determined using samples of 5% H_2O in D_2O.

RESULTS AND DISCUSSION

As shown in the calculated field map in Figure 3B, the field variations in the sample volume can be largely eliminated by surrounding it with carefully designed additional features, which are filled with a fluid with susceptibility mismatch of opposite sign. In the simplest case, the compensation fluid is air (χ_V=+0.05 ppm). However, in working with biological samples we can expect a range of sample magnetic susceptibilities, which would require either i) a substitute compensation fluid or ii) an additive material in the sample such as $CuSO_4$. In the present work, the susceptibility of the sample was altered systematically by adding (paramagnetic) $CuSO_4$. The resulting field distributions were measured using a B0 field imaging sequence.

Figure 4 shows the response of the experimental field maps indeed to adding $CuSO_4$. Fig. 4 (top) shows a B0 field image of a chip with a square sample chamber of 4 x 4 mm size and 150 µm depth filled with a solution of $CuSO_4$ in H_2O. At higher Cu concentration, corresponding to a 1.5 ppm mismatch in susceptibility, the same chip exhibits severe field variations (center). Surrounding the sample chamber with an air-filled structure as shown in Fig. 3 largely eliminates the field variations, as shown in Fig. 4 (bottom).

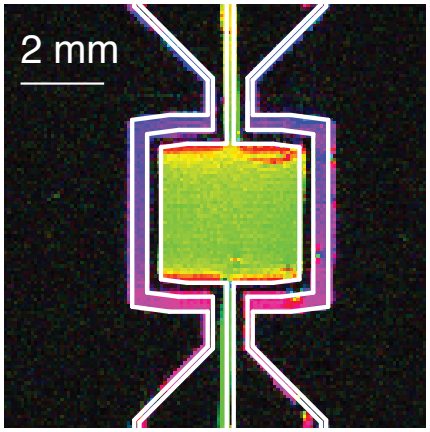

Figure 5: *Microfluidic chip with serviceable compensation structure allowing for stronger or weaker susceptibility mismatching state depending on sample type.*

One-dimensional field maps are plotted versus $CuSO_4$ concentration in figure 4 to highlight the effect of a compensation structure. The curvature of the field maps are positive at 0 mMol $CuSO_4$ resulting from interface of the paramagnetic PMMA and more diamagnetic sample (H_2O in this case). As the $CuSO_4$ concentration of the sample fluid is increased the magnetic susceptibility of the two materials can be matched to form a linear profile with no susceptibility jumps. Adding in a third material in the compensation structure will shifts this relationship, as expected. For example, without the compensation structure, the curvature of the field distribution in the center of the chip vanishes at a $CuSO_4$ concentration of 11 mM. With the compensation structure (which, in effect, makes the chip "more paramagnetic"), a flat profile is only achieved around 44 mM $CuSO_4$. Sharp spectral lines are obtained from flat field profiles. In practice, adding paramagnetic ions to the sample may not be a viable option due to their toxicity and/or their relaxivity. However, the experiments shown here used PMMA for the chip material for ease of fabrication. The susceptibility of PMMA lies slightly to the paramagnetic side of water. If, by contrast, the chip material is more diamagnetic than the sample, a flat field profile can be achieved by simply chosing the correct width of the compensation structure. Alternatively, the compensating structure can be filled with a more diamagnetic or paramagnetic material as required. Figure 5 shows a serviceable compensation structure chip where the surrounding volume can be filled with any working fluid.

CONCLUSIONS

We have shown that magnetic field distortions due to susceptibility mismatch in microfluidic chips can be corrected by appropriately designed on-chip compensation structures. These can be fabricated at the same time as the fluidic network. This principle of compensating susceptibility mismatches by adding features to the chip design is broadly applicable.

REFERENCES

1. Lindon, J., Nicholson, J., Holmes, E., & Everett, J. Metabolomics: metabolic processes studied by NMR spectroscopy of biofluids. *Concepts in Magnetic Resonance,* **12**, 289-320. (2000);
2. Vlad Badilita , Robert Ch. Meier , Nils Spengler , Ulrike Wallrabe , Marcel Utz and Jan G. Korvink, Microscale nuclear magnetic resonance: a tool for soft matter research, *Soft Matter*, DOI 10.1039/C2SM26065D (2012);
3. Ryan, H., Song, SH., Zaß, A., Korvink, J., & Utz, M. Contactless NMR Spectroscopy on a Chip. *Analytical Chemistry*, **84**, 3696-3702. (2012);
4. Sakellariou, D., Le Goff, G. and Jacquinot, J.F., *Nature* **447**, 694–697 (2007)
5. Utz, M. and Monazami, R., *J. Magn. Reson.* **198**, 132–136 (2009)
6. Olson, D., Peck, T., Webb, A., Magin, R., and Sweedler, J.: *Science*, **270**, 1967-1970, (1995);
7. Trumbull, J., Glasgow, I., Beebe, D., and Magin, R.: *IEEE Trans. Biomed. Eng.*, **47**, 3–7 (2000);
8. Massin, C., Boero, G., Vincent, F., Abenhaim, J., Besse, P., and Popovic, R., *Sensors & Actuators: A.* **97**, 280–288, (2002);
9. Bart, J., Kolkman, A.J. , Oosthoek-de Vries, A.J. , Koch, K. , Nieuwland, P.J. ,Janssen, H. , van Bentum, J. , Ampt, K.A.M. , Rutjes, F.P.J.T. , Wijmenga, S.S., et al. Journal of the American Chemical Society, 131, 5014–5015, (2009);